

Multimaterial 3D Reconstruction of Beetle Flapping-Wing Mechanisms

Ryuma Niiyama, Yoshihiro Kawahara, and Yasuo Kuniyoshi

Graduate School of Information Science and Technology, The University of Tokyo, Japan

niiyama@isi.imi.i.u-tokyo.ac.jp

1 Introduction

Flight mechanisms of insects have attracted research interest from both biologists and robotics researchers. Flapping-wing flight is a method that affords efficient and agile steering in the air especially in small-scale flyers as well as a set of rotors of a quadcopter. Past studies have investigated the basic principle of the flapping mechanism of a honey bee[1], a fly[2], and other species[3]. An early artificial working model was developed to explain the action of articulating flapping mechanism of fly[4].

There have been efforts to reconstruct the flapping mechanisms for developing a micro aerial vehicle (MAV)[5]. The primary engineering approach for reproducing the flapping motion of insect flight is the use of a crank-rocker mechanism driven by an electric motor. However, a mechanism with gears and linkages ignores elastic structure of shell and wing base. The crank-rocker mechanism has a fixed amplitude. Studies on MAVs with flexible microhinges[6, 7] and resonant flapping wings[8] suggest that the integrated compliant structure is a key feature for efficient flapping flight.

The purpose of this study is to reconstruct compliant articulating structure of the beetle wing base directly from CT data. We expect to contribute to enhancing the understanding of insect flight and also to the development of MAV.

2 Materials and Methods

2.1 Micro CT system for Beetle Specimen

The specimen used in the study is the Japanese rhinoceros beetle (*Trypoxylus dichotomus*) (Fig.1A). The beetles are purchased from a live insect supplier (Dorcus Danke, Inc.). The beetles were deactivated by organic sol-

Table 1: The parameters of micro CT scanning.

Parameter	Value	unit
source-image distance (SID)	500	mm
source-object distance (SOD)	250	mm
number of views per rotation	600	
X-ray tube voltage	33	kV
tube current	136	μ A
voxel size	0.062	mm

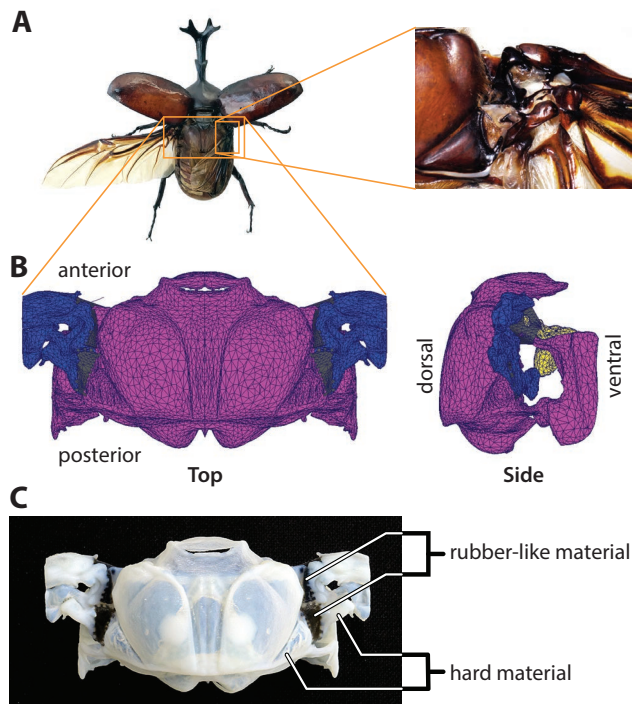


Figure 1: A: The beetle *Trypoxylus dichotomus*. Hard segments are joined by flexible membranous structure. B: Polygon mesh of the beetle metathorax obtained from micro CT data. C: Multi-material 3D printed shell.

vent poisoning and low-temperature treatment. The separated thorax shell was mounted on the micro CT stage after removal of muscles.

We used a microfocus X-ray CT system (inspeXio SMX-100CT, Shimadzu Co.) that is suitable for capturing the complex structure of animal body in high-resolution images. Parameters of the measurement of beetle thorax are shown in Table 1. Polygon meshes are generated from micro CT images by using a volume rendering software (VGStudio MAX, Volume Graphics GmbH) (Fig.1B).

2.2 Multimaterial 3D printing

Additive manufacturing technology allows three-dimensional printing of volumetric data by using polymer materials. We used an inkjet 3D printer that can print multiple materials simultaneously (Objet260 connex3, Stratasys Ltd.). A mixture of a hard resin material (VeroWhitePlus

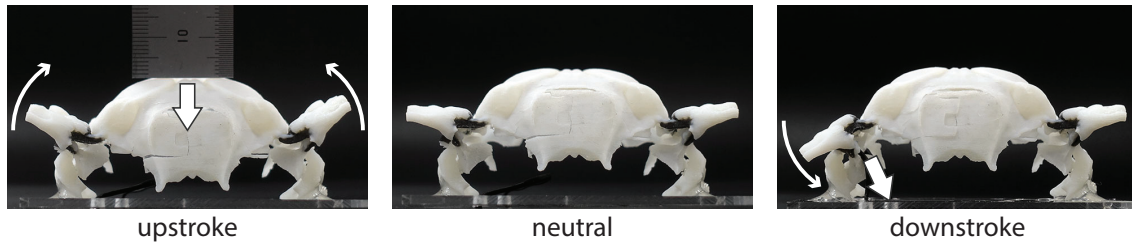


Figure 2: Response of compliant articulating structure to the displacement input. Bold arrow indicates input and thin arrow indicates resultant flapping motion. The upstroke experiment emulated the displacement of the shell caused by the indirect flight muscle: dorsoventral muscle (DVM). The upstroke experiment emulated the action of direct flight muscle: subalar and basalar muscle.

RGD835) and a rubber-like material (TangoBlackPlus FLX980) was used for mimicking plates. The rubber-like material was also used for replicating the flexible membranous structure between the plates (Fig.1C). Life-size printing of insect body is still the challenge. The printed shell is three times the size of the original.

3 Experiments

3.1 Setup

The multi-material 3D printer manufactured an artificial metathorax shell from the polygon mesh data. The scale of the mesh was magnified three times. The mesh was manually divided into sub-components and was assigned different materials. All the components were continuously combined. We focused on a metanotum (dorsal plate of metathorax), metapleuron (lateral plate) on each side, wing base, and connecting tissues (Fig.1). The artificial metathorax was bonded on an acrylic plate that functions as a metasternum (ventral plate). Instead of the contraction force of flight muscles, we input static displacement to the shell.

3.2 Upstroke

The dorsoventral muscle (DVM) that connects the notum and sternum causes upstroke motion of the wing in the case of beetle. The DVM is not directly linked to the wing base; therefore, it is called an indirect flight muscle. We observed that the artificial metathorax could reproduce the upstroke motion of the wing base (Fig.2). The upstroke angle is about 23° with about 3 mm displacement at the center of the notum plate. When the force to push the notum is removed, the wing base returns to the neutral position. This observation suggests that the compliant structure can support elastic oscillation around the equilibrium position.

3.3 Downstroke

Both direct and indirect flight muscles are related to the downstroke motion of the wing in the case of a beetle. In contrast to the upstroke mechanism, the detail of the downstroke mechanism is not well understood because of the complex deformation of the shells and the participation of multiple muscles. We focused on the subalar muscle and the basalar muscles directly connected to the wing base to see the articulation mechanism. We omitted the indirect muscle, the dorsal longitudinal muscle (DLM) that is also involved

in downstroke. We applied displacement to the two insertion lobes underneath the wing base with tensioned wire. We observed that the downstroke angle is about 39° with about 3 mm displacement (Fig.2). Unlike the upstroke motion induced by indirect flight muscles, each wing is depressed separately by direct flight muscles.

4 Conclusion

This study conducted a reconstruction compliant flapping mechanism of beetle by using a combination of additive manufacturing technique and a microfocus X-ray CT system. We present that multimaterial model can reproduce both upstroke and downstroke actions of the wing in good agreement with biological insight. There is an inherent articulation mechanism in the printed structure directly imported from CT data. The observed static amplitude of flapping is approximately a third of that shown by a living beetle. The results indicate that the beetle flapping employs a variable amplitude mechanism and utilizes dynamic resonance to amplify the range of motion.

5 Acknowledgement

This work was supported by the JST ERATO program, grant number JPMJER1501, Japan.

References

- [1] R.E. Snodgrass, "Anatomy of the Honey Bee," *Cornell University Press*, 1984.
- [2] E. G. BOETTIGER and E. FURSHPAN, "The Mechanics of Flight Movements in Diptera," *Biol. Bull.*, vol. 102, no. 3, pp. 200–211, 1952.
- [3] Robert Dudley, "The Biomechanics of Insect Flight: Form, Function, Evolution," *Princeton University Press*, 2000.
- [4] J.W.S. Pringle, "Insect Flight," *Cambridge University Press*, 1957.
- [5] D. Floreano, J.-C. Zufferey, M. V. Srinivasan, and C. Ellington, Eds., "Flying Insects and Robots," *Springer-Verlag*, 2010.
- [6] R. J. Wood, S. Avadhanula, M. Menon, and R. S. Fearing, "Microrobotics using composite materials: the micromechanical flying insect thorax," in *IEEE International Conference on Robotics and Automation (ICRA)*, vol. 2, pp. 1842–1849, 2003.
- [7] G. K. Lau, Y. W. Chin, J. T. W. Goh, and R. J. Wood, "Dipteran-insect-inspired thoracic mechanism with nonlinear stiffness to save inertial power of flapping-wing flight," *IEEE Trans. Robot.*, vol. 30, no. 5, pp. 1187–1197, 2014.
- [8] C. T. Bolsman, J. F. L. Goosen, and F. van Keulen, "Design Overview of a Resonant Wing Actuation Mechanism for Application in Flapping Wing MAVs," *Int. J. Micro Air Veh.*, vol. 1, no. 4, pp. 263–272, 2009.